

The weed managers guide to remote detection:

"Understanding opportunities and limitations of multi-resolution
and multi-modal technologies for remote detection of
weeds in heterogeneous landscapes"

Project Report

Identification and Mapping of Hawkweed Using Machine Learning
Techniques Applied to UAV-Acquired Multispectral and Hyperspectral
Imagery

Prepared by:

Narmilan Amarasingam

School of Electrical Engineering and Robotics
Queensland University of Technology

September 2022

Contents

List of Tables	IV
List of Figures.....	V
List of Acronyms	VI
1. Introduction.....	1
1.1 Project description.....	1
1.2 Background and Motivation.....	1
1.3 Hawkweed and their impacts.....	2
1.4 Objectives.....	3
2. Methodology.....	3
2.1 Site description.....	3
2.2 Ground truth data collection.....	5
2.2.1 McKenzie Region of New Zealand.....	5
2.2.2 Fifteen Mile Ridge in NSW	5
2.2.3 Long Plain in NSW	6
2.3 UAV data collection.....	7
2.3.1 McKenzie Region of New Zealand.....	7
2.3.1 Fifteen Mile Ridge in NSW	7
2.3.3 Long Plain in NSW	8
2.4 Software requirements for model training.....	9
2.5 Orthomosaics and raster alignment.....	9
2.6 Region of interest (ROI) for training and testing.....	10
2.7 Labelling.....	10
2.8 Training and testing of models	10
2.9.1 Multispectral imagery.....	10
2.9.2 Hyperspectral imagery.....	11
2.8 Model prediction and mapping.....	11
3. Results.....	11
3.1 Evaluation metrics.....	11
3.1.1 McKenzie Region of New Zealand.....	12
3.1.2 Fifteen Mile Ridge in NSW	13
3.1.3 Long Plain in NSW	14
3.2 Model prediction and mapping.....	15
3.2.1 McKenzie Region of New Zealand.....	15
3.2.2 Fifteen Mile Ridge in NSW	18
3.2.3 Long Plain in NSW	21

4. Discussion.....	22
5. Benefits of this project	23
6. Limitation of this work.....	23
7. Future works and Recommendations of this project.....	24
8. Conclusions	24
Publication.....	25
Acknowledgments.....	25
References.....	25

List of Tables

Table 1: GPS locations of study site 1 and site 2 in Fifteen Mile Ridge in New South Wales, Australia.....	4
Table 2: Summary of UAV multispectral image acquisition at McKenzie Region of New Zealand.	7
Table 3: Summary of UAV multispectral image acquisition in December 2020 at Fifteen Mile Ridge, NSW.....	7
Table 4: Summary of UAV multispectral image acquisition in January 2021 at Fifteen Mile Ridge, NSW.....	8
Table 5: Summary of UAV multispectral image acquisition in March 2021 at Fifteen Mile Ridge, NSW.....	8
Table 6: Flight mission details for multispectral and hyperspectral imagery captured between December 2020 and December 2021 at Long Plain in NSW.....	8
Table 7: Overall Accuracy of different ML models for 0.85cm/pixel at testing site	12
Table 8: Overall accuracy report of XGBoost for different spatial resolution at testing site.....	12
Table 9: Precision metrics of XGBoost for different spatial resolutions at the testing site.....	12
Table 10: Overall Accuracy of different machine learning models for 15m AGL.....	13
Table 11: Precision metrics of different machine learning models for 15m AGL.....	13
Table 12: Overall accuracy and precision metrics of XGBoost for different flight missions.....	13
Table 13: Overall accuracy and precision metrics of XGBoost for MSI and HSI.....	15

List of Figures

Figure 1: Appearance of mouse-ear hawkweed infestation in the field	3
Figure 2: Map depicting the location of Sawdon Station in the McKenzie Region of New Zealand.....	4
Figure 3: Map illustrating the geographical location of Fifteen Mile Ridge in New South Wales, Australia.....	4
Figure 4: Map showcasing the position of Long Plain in New South Wales, Australia.....	5
Figure 5: Illustration depicting blue ropes strung over patches of varying botanical composition and density of mouse-ear hawkweed at the study site of McKenzie Region of New Zealand.....	5
Figure 6: Ground truth locations (GTL) of orange hawkweed at the study site of Fifteen Mile Ridge in New South Wales (NSW), Australia.....	6
Figure 7: Illustration of ground truth locations at Long Plain in New South Wales (NSW), Australia.....	6
Figure 8: Testing at ground truth location number 11.....	16
Figure 9: Prediction results at different region of interest.....	16
Figure 10: Segmentation results at different GSD (cm/pixel).....	17
Figure 11: Segmentation results for site 01- December 2020 at different AGL.....	18
Figure 12: Segmentation results for site 01- January 2021 at different AGL	18
Figure 13: Segmentation results for site 01- March 2021 at different AGL.....	19
Figure 14: Segmentation results for site 02- December 2020 at different AGL.....	19
Figure 15: Segmentation results for site 02- January 2021 at different AGL	20
Figure 16: Segmentation results for site 02- March 2021 at different AGL.....	20
Figure 17: Segmentation results for temporal variation of site 1 at 15m AGL.....	21
Figure 18: Segmentation results at different AGL.....	21
Figure 19: Comparison of MSI and HSI prediction	22

List of Acronyms

ARI1	: Anthocyanin Reflectance Index 1
ARI2	: Anthocyanin Reflectance Index 2
ARVI	: Atmospherically Resistant Vegetation Index
CoP	: Community of Practice
CRI1	: Carotenoid Reflectance Index 1
CRI2	: Carotenoid Reflectance Index 2
CSU	: Charles Sturt University
DT	: Decision Tree
EVI	: Enhanced Vegetation Index
ExG	: Excess Green
GCI	: Green Chlorophyll Index
GCI	: Green Chlorophyll Index
GNDVI	: Green Normalised Difference Vegetation Index
GNDVI	: Green Normalised Difference Vegetation Index
GSD	: Ground Sampling Distance
GTL	: Ground Truth Location
KNN	: K-Nearest Neighbours
ML	: Machine Learning
MRENDVI	: Modified Red Edge Normalised Difference Vegetation Index
MRESR	: Modified Red Edge Simple Ratio
MSAVI	: Modified Soil-Adjusted Vegetation Index
NDRE	: Normalised Difference Red Edge Index
NDVI	: Normalised Difference Vegetation
PRI	: Photochemical Reflectance Index
QUT	: Queensland University of Technology
RF	: Random Forest
RGB	: Red Green Blue
RGRI	: Red Green Ratio Index
ROI	: Region of Interest
SICI	: Structure Insensitive Pigment Index
SRI	: Simple Ratio Index
SVC	: Support Vector Classification
UAV	: Unmanned Aerial Vehicle
VI	: Vegetation Index
VREI1	: Vogelmann Red Edge Index 1
WBI	: Water Band Index

1. Introduction

1.1 Project description

The project, entitled "The weed managers guide to Remote Detection: Understanding the opportunities and limitations of multi-resolution and multi-modal technologies for remote detection of weeds in heterogeneous landscapes", aims to investigate opportunities for cost-effective use of multi-resolution red, green, blue (RGB), multispectral (MS) and hyperspectral (HS) technologies across various airborne platforms (Unmanned aerial vehicle (UAV), manned aircraft, satellite), paired with multi-modal machine learning (ML) analyses to identify weeds in heterogeneous landscapes. In this component study, the nationally significant weed: yellow hawkweed (*Pilosella aurantiaca*) and mouse-earhawkweed (*Pilosella officinarum*), were used to test whether UAV-based MS and HS imagery and automated detection algorithms could feasibly detect the weed and such a process be used by weed managers. Remotely sensed imagery was combined with on-ground field assessments to develop a predictive model of hawkweed detection for the purpose of hawkweed management. The project aims to grow extensive national partner networks and to develop a national community of practice (CoP) to share learnings and advice on the remote detection of weeds. This research will inform the development of an information portal for weed managers to understand the opportunities and limitations of remote detection technologies in complex landscapes. The research was undertaken jointly by accomplished researchers in this field from Charles Sturt University (CSU) and Queensland University of Technology (QUT), in collaboration with NSW National Parks and Wildlife Service (Department of Planning and Environment) (NPWS), bringing a diverse and skilled team to the challenge.

1.2 Background and Motivation

Invasive plants, commonly referred to as weeds, have the capacity to outcompete native flora and fauna, posing threats to both agricultural productivity and natural environments [1], [2]. Invasive plant species can be categorised into two distinct groups [1] including agricultural weeds and environmental weeds. Agricultural weeds pose significant threats to crop fields, horticultural settings, and pasturelands, often impeding agricultural productivity. Moreover, certain agricultural weeds possess toxic properties, posing risks to both humans and livestock [1]. On the other hand, environmental weeds threaten natural ecosystems by influencing upon native plant communities [1]. Their invasive nature allows them to outcompete indigenous species, leading to a decline in plant diversity and the degradation of habitats crucial for native fauna. Weed control is essential to protect biodiversity and for crop and pasture management, as ineffective weed control leads to lower yields and inferior product quality and impacts the environment [3]. Conventional surveillance methods (e.g., field surveys) for invasive plant species are time-consuming, risky, and costly, resulting in a paucity of quantitative data regarding weed distribution in Australia. Surveillance is a crucial aspect of biosecurity since it enables the early discovery of invasive species and facilitates the comprehension of the spread of pests, weeds, and diseases. Although remote sensing (RS) is being investigated as a weed detection tool for various weeds in different landscapes across Australia and internationally, it has been met with mixed success due to difficulties associated with the low spatial and spectral resolution, access to expensive and complex technology, and a limited understanding of the utilisation of the

technology for detection of weeds inhabiting various terrain. The creation of analytics utilising cutting-edge spectral imaging systems in the hawkweed detection model will facilitate the testing of the limits of the most recent technology for future application to other weeds in heterogeneous settings.

RS can efficiently and cost-effectively acquire geospatial data over expansive areas [4]. The use of RS and airborne imaging to assess weeds is a technology that is expanding globally but is still in its infancy in many locations. Recently, RS has been successfully utilised to detect hawkweeds during flowering in Kosciuszko National Park, Australia [5]. However, this approach relies on a survey occurring in the brief flowing period and is insufficient for detecting weeds in their vegetative stages when spectral signatures tend to be less recognisable from other green plants. The application of ML methods and analysis to remotely sense colour, MS, and thermal imaging has been identified as a potentially cost-effective strategy for locating diverse weed species in the field [6]. Successful ML algorithms have been deployed to capture UAV images consisting of numerous spectral bands to identify weed infestations [7]. Alternatively, in the visible spectrum region, ML techniques have made it possible to extract many scene elements that can be employed for object discrimination [8]. Developing optimal methodologies for utilising RS for landscape weed detection combined with a progressive learning community and educational guidelines will make these technologies more accessible to land managers in future. Guidelines will summarise the advantages and disadvantages of remote weed detection, and decision support will be provided to enable land managers to target their investments and maximise the use of current technology. The CoP will facilitate collaboration in this rapidly evolving subject by connecting researchers and end-users.

1.3 Hawkweed and their impacts

The invasion of exotic species is one of the greatest threats to the persistence of biodiversity in natural ecosystems throughout the world. Hawkweeds (*Hieracium spp.*) are perennial herbs that are serious environmental and agricultural weeds in many temperate and subalpine areas of the world [9]. It is native to Europe and Asia [10] but these biological traits have contributed to hawkweeds becoming major weeds in the United States of America, Canada, Japan, and New Zealand [11]. There are different hawkweed species in different geographical locations [12]. Mouse-ear hawkweed (*Pilosella officinarum*) is another prohibited matter in New South Wales (NSW) due to its invasive characteristics, particularly in alpine regions. Similar to orange hawkweed, it forms dense mats, outcompeting native vegetation, reducing food and habitat for native animals, and impacting grazing productivity [10], [13]. Recognisable by its small size, yellow daisy-like flowers, and hairy leaves arranged in a rosette, mouse-ear hawkweed reproduces through seeds and vegetative spread via stolons and rhizomes [10], [13]. Figure 1 illustrates the appearance of a mouse-ear hawkweed infestation in the field. Orange hawkweed (*Pilosella aurantiaca*) is a prohibited matter in NSW due to its highly invasive nature and threat to biodiversity and agriculture [14]. With dense stands of thousands of plants per square meter, it outcompetes native vegetation, reduces food and habitat for native animals, and invades pastures, leading to decreased productivity. Identified by its small size, orange daisy-like flowers, and hairy leaves arranged in a rosette, orange hawkweed reproduces rapidly through seeds and vegetative spread via stolons and rhizomes [14]. The hawkweed population alter the soil's chemical properties, such as soil organic matter, nitrogen content, acidity, and exchangeable cations [15]. Also, it prevents the germination and growth of other plants by producing biochemicals and

secreting them into the surrounding soil [10]. Therefore, early detection generally requires a substantial upfront investment, while delayed detection can cause otherwise considerable, if not devastating, damages [16].



Figure 1: Appearance of mouse-ear hawkweed infestation in the field. (Photo credit: Mark Hamilton, NSW Department of Planning and Environment)

1.4 Objectives

- To propose a technique for detecting hawkweed in MS and HS imagery captured by UAVs and compares different ML classification algorithms at different spatial resolutions.
- To provide learning opportunities on remote weed detection practices and methods.
- To support effective weed biosecurity and management focused on building capacity and capability in remote weed detection.

2. Methodology

2.1 Site description

Data collection for the Hawkweed UAV imagery spanned three distinct sites in Australia and New Zealand. Sawdon Station, located in the McKenzie Region of New Zealand ($170^{\circ}18'30.80"E$ and $44^{\circ}8'39.17"S$), was surveyed in January 2021 (Figure 2), targeting mouse-ear hawkweed. In New South Wales, Australia, the first site, Fifteen Mile Ridge (Figure 3), was monitored between December 2020 and March 2021, focusing on orange hawkweed. The second site, Long Plain, also in New South Wales, Australia ($148^{\circ}35'13.00"E$ and $35^{\circ}41'31.43"S$), underwent data collection from December 2020 to December 2021 (Figure 4), primarily addressing orange hawkweed. These sites offered diverse geographical contexts for acquiring hawkweed UAV MS and HS

imagery, facilitating comprehensive analysis of vegetation dynamics across different regions and timeframes.



Figure 2: Map depicting the location of Sawdon Station in the McKenzie Region of New Zealand.

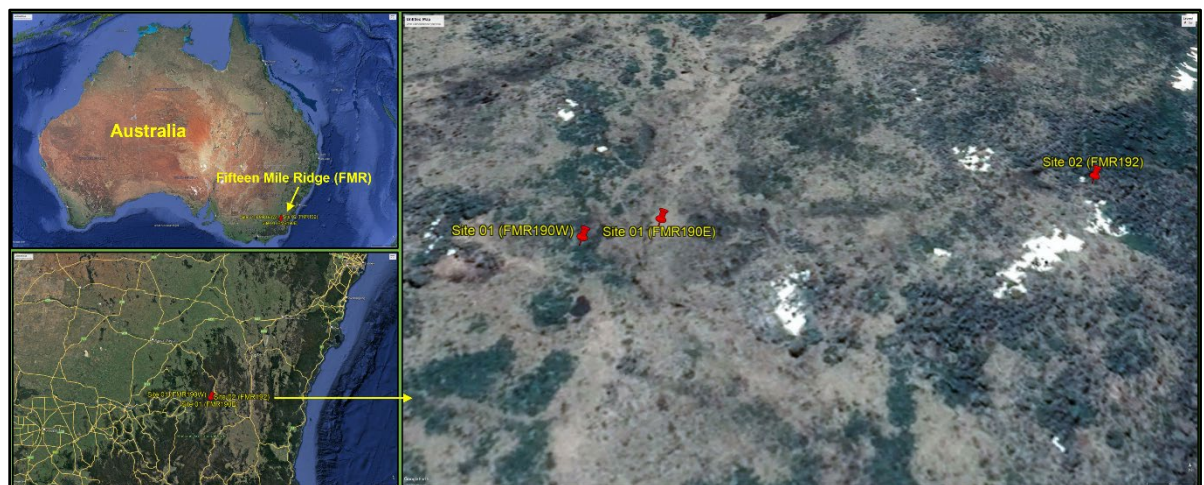


Figure 3: Map illustrating the geographical location of Fifteen Mile Ridge in New South Wales, Australia.

Table 1: GPS locations of study site 1 and site 2 in Fifteen Mile Ridge in New South Wales, Australia.

Site	Latitude	Longitude
Site 01 (FMR190W)	36° 0'52.91"S	148°24'27.84"E
Site 01 (FMR190E)	36° 0'52.44"S	148°24'29.15"E
Site 02 (FMR192)	36° 0'51.07"S	148°24'37.79"E

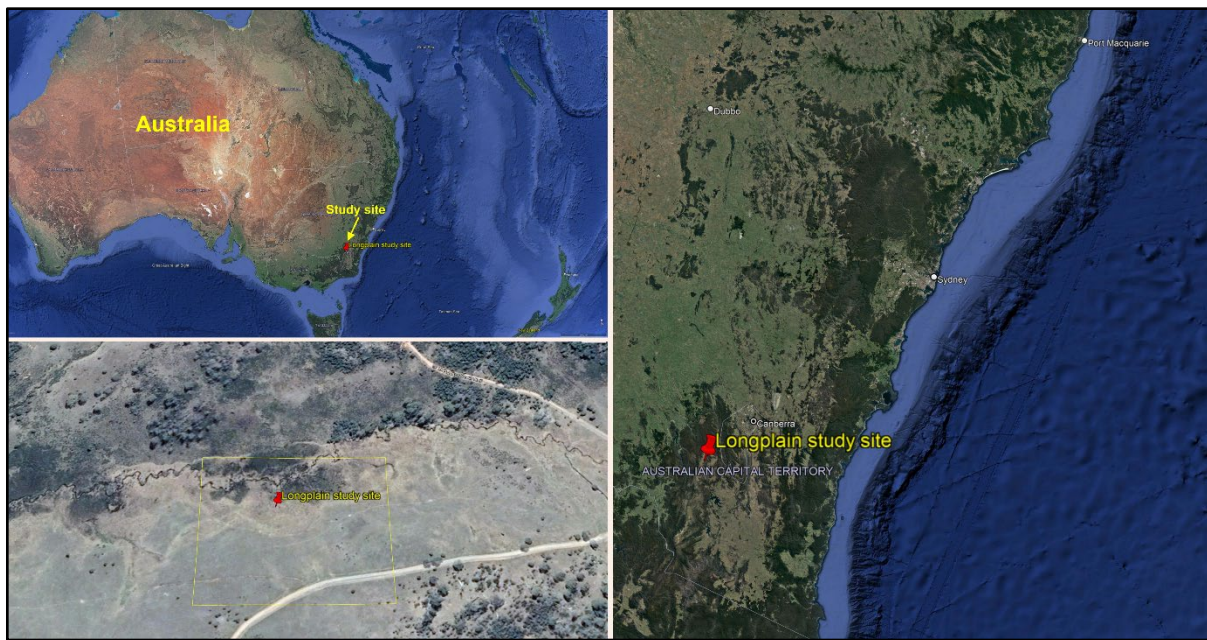


Figure 4: Map showcasing the position of Long Plain in New South Wales, Australia.

2.2 Ground truth data collection

2.2.1 McKenzie Region of New Zealand

The blue ropes were strung over patches of varying botanical composition and density of mouse-ear hawkweed to assist in the confirmation of all species captured in the imagery (Figure 5). Ground disturbance of mouse-ear hawkweed and other vegetation within the patches, as well as weather conditions at the study site, were recorded.

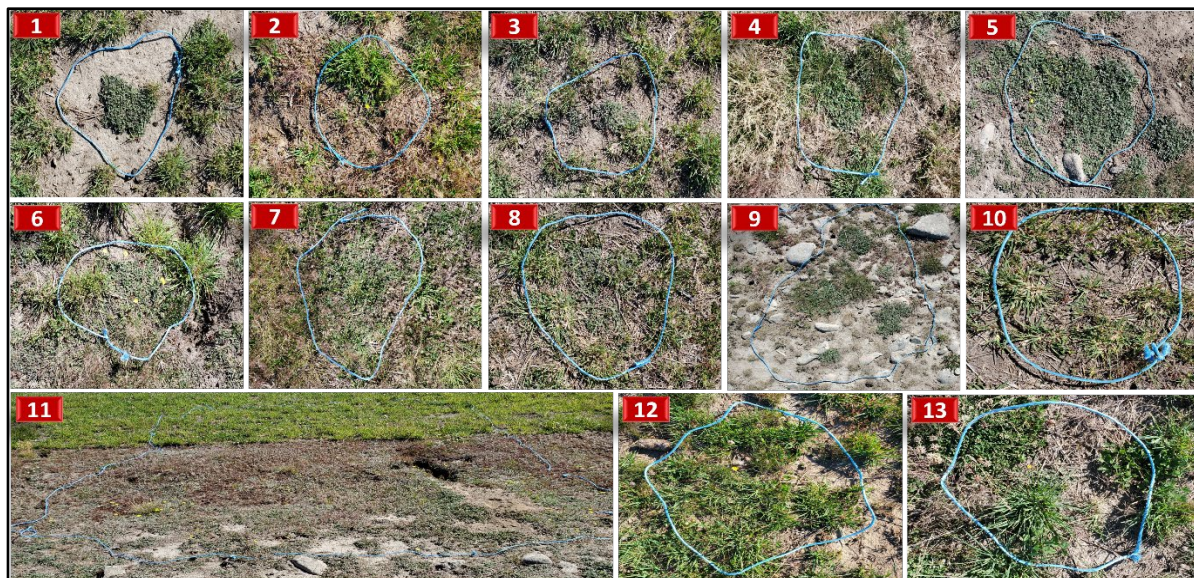


Figure 5: Illustration depicting blue ropes strung over patches of varying botanical composition and density of mouse-ear hawkweed at the study site of McKenzie Region of New Zealand.

2.2.2 Fifteen Mile Ridge in NSW

The blue ropes were placed over regions with varying botanical composition and density of hawkweed to assist in the confirmation of all species captured in the imagery. Ground photos of

each ground truth location (GTL) were acquired as reference images, and GTL characteristics were recorded, including GPS location, plant species composition, plant height, species phenological stage, and percentage of ground disturbance. Figure 6 depicts the ground truth locations at the study site in Fifteen Mile Ridge.



Figure 6: Ground truth locations (GTL) of orange hawkweed at the study site of Fifteen Mile Ridge in New South Wales (NSW), Australia.

2.2.3 Long Plain in NSW

The white plastic reference quadrats (1m x 1m) were placed across the site in areas representing variable botanical composition and orange hawkweed density (Figure 7). Ground images of each quadrat were captured using a Nikon D600 DSLR camera as reference images, and quadrat features were recorded, including GPS location, plant species composition, plant height, species phenological stage, and percentage of ground disturbance. Additionally, cloud cover, wind speed, humidity, temperature, and altitude were documented.



Figure 7: Illustration of ground truth locations at Long Plain in New South Wales (NSW), Australia, featuring white plastic reference quadrats aiding in species validation within imagery.

2.3 UAV data collection

2.3.1 McKenzie Region of New Zealand

The UAV flight missions were conducted using a MS MicaSense Altum sensor mounted on DJI Matrice 600 UAV between 12:00 and 14:00 New Zealand local time on 30-31 January 2021 under sunny conditions. The MicaSense Altum sensor detects five reflectance bands of Blue, Green, Red, Red Edge, and Near Infrared with the wavelengths of 475.0nm, 560.0nm, 668.0nm, 717.0nm, and 842.0nm, respectively. The imagery was collected at multiple spatial resolutions to determine the ideal resolution for the detection of mouse-ear hawkweed, being cognisant that lower-resolution imagery is cheaper to collect and allows greater areas to be surveyed. Table 2 provides information regarding image capture, including above ground level (AGL), ground sampling distance (GSD), speed, overlap, take-off time, and mission dates.

Table 2: Summary of UAV multispectral image acquisition at McKenzie Region of New Zealand.

Flight mission No	AGL (m)	GSD (cm/pixel)	Speed (ms ⁻¹)	Overlapping	Take off time	Date of mission
1	15	0.65	2	75%	12.10	30.01.2021
2	20	0.86	2.2	75%	12.47	30.01.2021
3	25	1.10	2.8	75%	13.17	30.01.2021
4	30	1.30	3.3	75%	13.32	30.01.2021
5	35	1.50	4	75%	13.35	30.01.2021
6	40	1.73	4.5	75%	13.06	30.01.2021
7	45	1.95	5	75%	12.37	30.01.2021

AGL: Above Ground Level; GSD: Ground Sampling Distance; Take off time: NZ local time

2.3.1 Fifteen Mile Ridge in NSW

The UAV flight missions were conducted using a MicaSense Altum sensor mounted on DJI Matrice 300 on a sunny day. Tables 3 ,4 and 5 provide information regarding image capture, including AGL, and GSD in different period between December 2020 and March 2021.

Table 3: Summary of UAV multispectral image acquisition in December 2020 at Fifteen Mile Ridge, NSW.

Site	Flight No	AGL	GSD (cm/pixel)
1	1	15m	0.71cm
	2	20m	0.96cm
	3	25m	1.17cm
	4	30m	1.40cm
	5	35m	1.64cm
	6	40m	1.87cm
	7	45m	2.08cm
2	1	15m	0.76cm
	2	20m	1.00cm
	3	25m	1.24cm
	4	30m	1.47cm
	5	35m	1.66cm
	6	40m	1.86cm
	7	45m	2.00cm

AGL: Above Ground level; GSD: Ground Sampling Distance

Table 4: Summary of UAV multispectral image acquisition in January 2021 at Fifteen Mile Ridge, NSW.

Site	Flight No	AGL	GSD (cm/pixel)
1	1	15m	0.71cm
	2	20m	0.93cm
	3	25m	1.14cm
	4	30m	1.37cm
	5	35m	1.60cm
	6	40m	1.85cm
	7	45m	2.06cm
2	1	15m	1.12cm
	2	20m	1.32cm
	3	25m	1.61cm
	4	30m	1.87cm
	5	35m	2.15cm
	6	40m	2.33cm
	7	45m	2.57cm

AGL: Above Ground level; GSD: Ground Sampling Distance

Table 5: Summary of UAV multispectral image acquisition in March 2021 at Fifteen Mile Ridge, NSW.

Site	Flight No	AGL	GSD (cm/pixel)
1	1	15m	0.98cm
	2	20m	1.25cm
	3	25m	1.44cm
	4	30m	1.67cm
	5	35m	1.89cm
	6	40m	2.12cm
	7	45m	2.34cm
2	1	15m	1.41cm
	2	20m	1.61cm
	3	25m	1.89cm
	4	30m	2.08cm
	5	35m	2.34cm
	6	40m	2.53cm
	7	45m	2.76cm

AGL: Above Ground level; GSD: Ground Sampling Distance

2.3.3 Long Plain in NSW

The UAV flight missions were conducted using a MS (MicaSense altum (5 bands)) and HS (Specim AFX VNIR covering 400-1000nm of the electromagnetic spectrum (448 bands)) cameras mounted on DJI Matrice 300 and DJI Matrice 600 respectively. Table 6 provides information regarding image capture, including AGL and GSD.

Table 6: Flight mission details for multispectral and hyperspectral imagery captured between December 2020 and December 2021 at Long Plain in NSW.

Month	Type of imagery	Flight mission No	AGL (m)
December, 2020	MSI	1	15
		2	20
		3	25
		4	30

		5	35
		6	40
		7	45
January, 2021	MSI	1	15
		2	20
		3	25
		4	30
		5	35
		6	40
		7	45
		1	15
March, 2021	MSI	2	20
		3	25
		4	30
		5	35
		6	40
		7	45
		1	15
December, 2021	HSI	1	50

AGL: Above Ground level; GSD: Ground Sampling Distance; MSI: Multispectral imagery, HSI: Hyperspectral imagery

2.4 Software requirements for model training

These studies were conducted utilising several software applications and Python libraries. Agisoft Metashape (Version 1.6.6) was used for MS image analysis to process, filter, and orthorectify images. A collection of images was recovered from cropped sections and then labelled using QGIS (Version 3.2.0). Visual Studio Code (VS Code) 1.70.0 was utilised as the source code editor to develop ML algorithms using Python 3.8.10. Several libraries were utilised for data processing and ML, including Geospatial Data Abstraction Library (GDAL) 3.0.2, Extreme Gradient Boosting (XGBoost) 1.5.0, Scikit-learn 0.24.2, OpenCV 4.6.0.66, and Matplotlib 3.0. The data analysis was conducted using a custom Python script, which is available in our [GitHub repository](#). This script includes all the necessary functions to replicate the analysis.

2.5 Orthomosaics and raster alignment

Initial image processing for all sites involved generating orthomosaics using data from multiple flight missions. In New Zealand, orthomosaic rasters from various missions with ground sample distances (GSD) ranging from 0.86 to 1.95 cm/pixel were georeferenced with the highest resolution raster image (0.65 cm/pixel) through pixel-level alignment to avoid ground truth labelling for all flights. Similar processing occurred for the Fifteen Mile Ridge site, where orthomosaic rasters from missions with altitudes ranging from 20m to 45m were aligned with the highest resolution image from the 15m flight mission. This approach aimed to achieve pixel-level alignment between all lower resolution rasters. Similarly, at Long Plain, orthomosaic rasters from missions with altitudes ranging from 20m to 45m were georeferenced with the highest resolution raster image from the 15m flight mission to achieve pixel-level alignment. Additionally, the HS image was aligned with a high-resolution RGB image (GSD at 0.22cm per pixel) for labelling purposes.

2.6 Region of interest (ROI) for training and testing

Based on ground truth information obtained from each site, regions of interest (ROIs) were extracted for training and testing purposes. At the New Zealand site, ROIs were delineated based on mouse-ear hawkweed distribution. Similarly, at Fifteen Mile Ridge, ROIs were identified considering orange hawkweed prevalence across Site 01 and Site 02. At Long Plain, ROIs were defined to encompass areas with mouse-ear hawkweed presence. These ROIs served as the basis for training and testing models to accurately classify and analyse hawkweed distribution and dynamics within each respective site.

2.7 Labelling

High resolution RGB and respective georeferenced MS and HS imageries were loaded into QGIS. A new shapefile for training and testing ROIs was created with a polygon geometry type and an attribute field called class id of type Integer. Training data were digitised by selecting the new shapefile layer, toggling editing mode, and using the appropriate tool to draw polygons around areas representing different classes of vegetation or hawkweed density. Class IDs were assigned by entering the integer value for the class id attribute in the dialog box that appeared during polygon creation. In the McKenzie Region of New Zealand, integer values were assigned as follows: 1 for mouse-ear hawkweed flower, 2 for mouse-ear hawkweed foliage, 3 for other vegetation, and 4 for non-vegetation. For Fifteen Mile Ridge, values of 1, 2, and 3 represented orange hawkweed, other vegetation, and non-vegetation, respectively. At Long Plain, QGIS was used to label the December 2020 multispectral raster dataset with integers: 1 for orange hawkweed foliage, 2 for orange hawkweed flower, 3 for other vegetation, 4 for other flowers, and 5 for non-vegetation. The January 2021 and March 2021 datasets were excluded due to the lack of ground truth information. For HS image processing, two classes were assigned: 1 for orange hawkweed foliage and 2 for other vegetation, as orange hawkweed flowers were not identifiable due to their size being smaller than the pixel size (3.5 cm per pixel) of the MS image. The labeled dataset (McKenzie Region of New Zealand) is available for reference and validation purposes. Access the ground truth labeling data [here](#).

2.8 Training and testing of models

2.9.1 Multispectral imagery

Numerous processes are involved in constructing algorithms, including loading, pre-processing, fitting the classifier to the data, and prediction. The processing phase transforms the read input into a set of features, which the classifier subsequently analyses. Five reflectance bands are loaded into the algorithm to increase detection rates by calculating spectral vegetation indices (VI). The Normalised Difference Vegetation Index (NDVI), Green Normalised Vegetation Index (GNDVI), Normalised Difference Red Edge Index (NDRE), Green Chlorophyll Index (GCI), Modified Soil-Adjusted Vegetation Index (MSAVI), and Excess Green (ExG) were calculated for this method to improve the input features and accuracy of the models. All five reflectance bands and the computed VIs are input characteristics. The ground-based assessments' labelled regions are exported from QGIS and placed into an array. Filtered pixel-wise data were randomly divided into a training array (75%) and a testing array (25%). Initially, the highest resolution raster dataset (15m) was fitted into many ML classifiers, including XGBoost, SVC, RF, DT, and KNN, to detect the hawkweed at the sites. Then, the selected ML classifier was chosen based on the model's

accuracy to train the other imageries with different resolutions. For detailed technical information regarding the model training and testing process, including code implementation and experiment results, please visit our [GitHub repository: Model Training and Testing Details](#).

2.9.2 Hyperspectral imagery

Similar to MS image processing methodology, the model was developed using a HS image at 50m AGL for December 2021 dataset. Eighteen VIs were used to improve the detection accuracy of the model. Altogether, 466 input features (448 HS bands and 18 VIs). Normalised Difference Vegetation Index (NDVI), Green Normalised Difference Vegetation Index (GNDVI), Modified Soil Adjusted Vegetation Index (MSAVI), Enhanced Vegetation Index (EVI), Photochemical Reflectance Index (PRI), Simple Ratio Index (SRI), Atmospherically Resistant Vegetation Index (ARVI), Modified Red Edge Simple Ratio (MRESR), Modified Red Edge Normalised Difference Vegetation Index (MRENDVI), Vogelmann Red Edge Index 1 (VREI1), Structure Insensitive Pigment Index (SIPI), Green Chlorophyll Index (GCI), Red Green Ratio Index (RGRI), Carotenoid Reflectance Index 1 (CRI1), Carotenoid Reflectance Index 2 (CRI2), Anthocyanin Reflectance Index 1 (ARI1), Anthocyanin Reflectance Index 2 (ARI2), and Water Band Index (WBI) were used in this HS model training.

2.8 Model prediction and mapping

During the prediction stage, unlabelled pixels are processed using the most effective classifier, and their values are shown in the same 2D spatial image from the orthorectified MS an HS cube. The recognised pixels of each image are then coloured differently and saved in TIF format, which geographic information systems (GIS) platforms can read. Finally, the predicted map was aligned with the high resolution RGB imagery to confirm the accuracy of the expected outcome by hawkweed specialists.

3. Results

3.1 Evaluation metrics

Overall accuracy and precision were used to evaluate the model's testing performance in this study. Confusion metrics and classification reports were established to compare the models and evaluate the detection performance of the best model. Evaluation descriptors, including true positive (TP), false positive (FP), true negative (TN), and false-negative (FN) were used to construct the confusion matrix (Equation (1)) and then to determine the overall accuracy (Equation (2)) and precision (Equation (3)).

$$\text{Confusion Matrix} = \begin{bmatrix} TP & FP \\ FN & TN \end{bmatrix} \quad (1)$$

$$\text{Overall Accuracy} = \frac{TP+TN}{TP+TN+FP+FN} \quad (2)$$

$$\text{Precision} = \frac{TP}{TP+FP} \quad (3)$$

3.1.1 McKenzie Region of New Zealand

Results of the analysis show an overall accuracy of 98% was attained in with XGBoost to detect mouse-ear hawkweed at the site. This occurred despite other models, namely SVC, RF, DT, and KNN, obtaining an overall accuracy of 94%, 96%, 93%, and 93%, respectively, as shown in Table 4. Note, these accuracy values need to be interpreted in the context of the size of the dataset and the environment where imagery was captured, being a disturbed pasture with high mouse-ear hawkweed abundance and overall low species diversity and hence lower likelihood of species that could be confused with hawkweed. Finally, the XGBoost model was selected as the best algorithm to train the other spatial resolution of raster images for hawkweed detection. Table 7 shows the overall accuracy for classifying the hawkweed flower, hawkweed foliage, other vegetation, and non-vegetation for different spatial resolutions. As expected, the 0.65cm/pixel (15m AGL) mission obtained the highest overall accuracy. Also, overall accuracy of 91%, 96%, 96%, 96%, and 94% were attained for GSD at 0.86, 1.10, 1.30, 1.50, 1.73, 1.95 cm/pixel respectively (Table 8). Table 9 show the precision metrics of the XGBoost model for different spatial resolutions at the testing site to classify the hawkweed flower, hawkweed foliage, other vegetation, and non-vegetation. A precision of 100% was obtained for 0.65, 0.86, 1.50, 1.73, and 1.95 cm/pixel flight missions to detect the hawkweed flowers in the validation site. However, the lowest precision value of 96% was obtained at 1.10cm/pixel (25m flight height). Meanwhile, the highest precision of 93% was attained during a 15m flight mission at 0.65cm/pixel GSD for detecting the hawkweed foliage, and a 25m flight mission (1.10cm/pixel) obtained the lowest. However, 90% and 92% of precision were achieved at flight heights of 1.73 and 1.95cm/pixel of GSD, respectively. For a comprehensive overview of the detailed results obtained from our experiments, including tables, charts, and analysis, please refer to our [GitHub repository: Detailed Results](#).

Table 7: Overall Accuracy of different ML models for 0.85cm/pixel at testing site

XGBoost	SVC	RF	DT	KNN
98%	94%	96%	93%	93%

Extreme Gradient Boosting (XGBoost); Support Vector Classification (SVC); Random Forest (RF); Decision Tree (DT); K-nearest neighbours (KNN)

Table 8: Overall accuracy report of XGBoost for different spatial resolution at testing site.

Flight No	GSD (cm/pixel)	Overall accuracy for classification of Hawkweed foliage, Hawkweed flowers, Other vegetations, and Non-vegetation (%)		
		Hawkweed flowers	Other vegetations	Non-vegetation
1	0.65		98	
2	0.86		91	
3	1.10		96	
4	1.30		96	
5	1.50		96	
6	1.73		96	
7	1.95		94	

Table 9: Precision metrics of XGBoost for different spatial resolutions at the testing site.

Flight No	GSD (cm/pixel)	Hawkweed flower (%)	Hawkweed foliage (%)	Other vegetation (%)	Non- vegetation (%)
1	0.65	100	93	97	100
2	0.86	100	80	82	100
3	1.10	96	79	94	99

4	1.30	99	86	94	100
5	1.50	100	87	92	100
6	1.73	100	90	92	100
7	1.95	100	92	88	100

3.1.2 Fifteen Mile Ridge in NSW

Tables 10 and 11 represent the overall accuracy and precision metrics for orange hawkweed detection in site 01 and site 02. The results revealed that metrics results from XGBoost, RF, and DT were not shown much difference for the detection of orange hawkweed.

Table 10: Overall Accuracy of different machine learning models for 15m AGL.

Mission period	Site	XGBoost	RF	DT
December 2020	Site 1	99%	96%	96%
	Site 2	94%	99%	99%
January 2021	Site 1	99%	99%	99%
	Site 2	99%	99%	99%
March 2021	Site 1	99%	98%	98%
	Site 2	99%	99%	99%

Extreme Gradient Boosting (XGBoost); Random Forest (RF); Decision Tree (DT)

Table 11: Precision metrics of different machine learning models for 15m AGL.

Mission period	Site	XGBoost	RF	DT
December 2020	Site 1	74%	79%	79%
	Site 2	87%	80%	80%
January 2021	Site 1	74%	77%	77%
	Site 2	78%	79%	79%
March 2021	Site 1	74%	78%	78%
	Site 2	75%	86%	86%

Table 12 shows the overall accuracy and precision metrics of the XGBoost model for different sites and different AGL and different time periods between December 2020 and March 2021. Overall accuracy for the detection of orange hawkweed ranged between 93% and 99%. Most of the precision metrics from different flight missions produced poor detection due to various reasons, such as the low amount of training samples and, poor quality of the MS images, poor ground truth information. Therefore, these reasons ultimately affected the labelling process and model performance. Based on the metrics, different AGLs were not affected by the orange hawkweed detection performance in this study. In addition to that, the detection performance of the march dataset was shown to be lowest than in other months because orange hawkweed was overlayed with other vegetation in the site. Therefore, the orange hawkweed class was not correctly identified in the MS raster during the labelling process.

Table 12: Overall accuracy and precision metrics of XGBoost for different flight missions.

Mission Period	Site	Flight No	AGL	Overall Accuracy in %	Precision for orange hawkweed detection in %
December, 2020	1	1	15m	99	74
		2	20m	97	79
		3	25m	95	67

January, 2021	1	4	30m	94	76
		5	35m	97	80
		6	40m	95	62
		7	45m	93	63
		1	15m	94	79
		2	20m	97	93
		3	25m	97	95
	2	4	30m	96	95
		5	35m	97	93
		6	40m	98	97
		7	45m	97	94
		1	15m	99	74
		2	20m	99	73
		3	25m	99	82
March, 2021	1	4	30m	99	84
		5	35m	98	73
		6	40m	99	83
		7	45m	99	72
		1	15m	99	78
		2	20m	96	81
		3	25m	99	82
	2	4	30m	99	80
		5	35m	98	85
		6	40m	98	85
		7	45m	97	85
		1	15m	99	74
		2	20m	98	69
		3	25m	97	57
	1	4	30m	97	55
		5	35m	97	52
		6	40m	97	51
		7	45m	99	76
		1	15m	99	73
		2	20m	97	69
		3	25m	97	83
	2	4	30m	97	75
		5	35m	97	65
		6	40m	97	60
		7	45m	97	48

3.1.3 Long Plain in NSW

The results (as shown in table 13) show that 96% of the overall accuracy of classifying the orange hawkweed, orange hawkweed flower, yellow flower from other vegetation, other vegetation, and non-vegetation was attained from the XGBoost model at 15m AGL to detect orange hawkweed at the site in December 2021. Also, the overall accuracy of 98%, 94%, 94%, 93%, and 95% was attained by 20m, 25m, 30m, 40m, and 45m, respectively, as shown in Table 13. The precision value of 73%, 94%, 96%, 96%, 80% and 94% was obtained by flight missions of 15m, 20m, 25m, 30m, 40m and 45m, respectively, to detect the orange hawkweed foliage. orange hawkweed flowers were detected by only the 15m and 20m flight missions at precision values of 81% and 62%, respectively. orange hawkweed flower detection was not developed from other flight missions due to the poor quality of the raster images and lack of ground truth information to train the XGBoost model. Due to the unavailability of ground truth information for January 2021 and

March 2021, detection models were not developed to identify the orange hawkweed. According to table 3, 98% of overall accuracy and 93% of precision value for hawkweed detection were obtained to classify the orange hawkweed and other vegetation from the XGBoost model in the HS image. Orange hawkweed flower was not detected by using HS data due to poor spatial resolution. It means that pixelwise classification for the orange hawkweed flower could not be developed because the actual size of the flower is less than the spatial resolution (3.5cm/pixel) of a HS raster image.

Table 13: Overall accuracy and precision metrics of XGBoost for MSI and HSI.

Period	Flight No	AGL	Imagery	Overall Accuracy in %	Precision for orange hawkweed detection in %	Precision for orange hawkweed flower detection in %
December 2020	1	15m	MSI	96	73	81
	2	20m		98	94	62
	3	25m		94	96	0
	4	30m		94	96	0
	5	35m		Missing data		
	6	40m		93	80	0
	7	45m		95	94	0
				Detection model was not developed due to no ground truth information for labelling the training data.		
January 2021	1	15m				
	2	20m				
	3	25m				
	4	30m				
	5	35m				
	6	40m				
	7	45m				
March 2021	1	15m				
	2	20m				
	3	25m				
	4	30m				
	5	35m				
	6	40m				
	7	45m				
December 2021	1	50m	HSI	98	93	NA

MSI: Multispectral imagery, HSI: Hyperspectral imagery

3.2 Model prediction and mapping

3.2.1 McKenzie Region of New Zealand

Figure 8 shows the prediction results at the validation site and most of the hawkweed flowers were detected using this model during the validation process. Figure 9 represents the model segmentation results with classes of hawkweed foliage, other vegetation, and non-vegetation at different GSD at a resolution of 0.65 cm/pixel using the XGBoost model. According to the prediction results as shown in Figure 9, hawkweeds were truly predicted in the pastureland (Figure 9d-f). Figure 10 represents the XGBoost model segmentation results with classes of hawkweed flower, hawkweed foliage, other vegetation, and non-vegetation at different GSD of

flight missions. To view the prediction results generated by our model, please visit the following link: [Prediction Results](#).

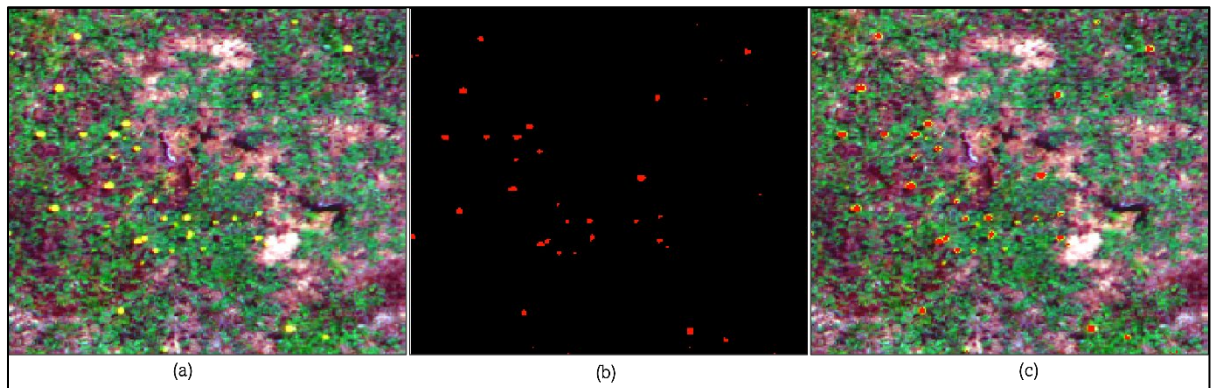


Figure 8: Testing at ground truth location number 11 (a) Actual multispectral image; (b) Prediction result; (c) Prediction results are overlayed with actual image.

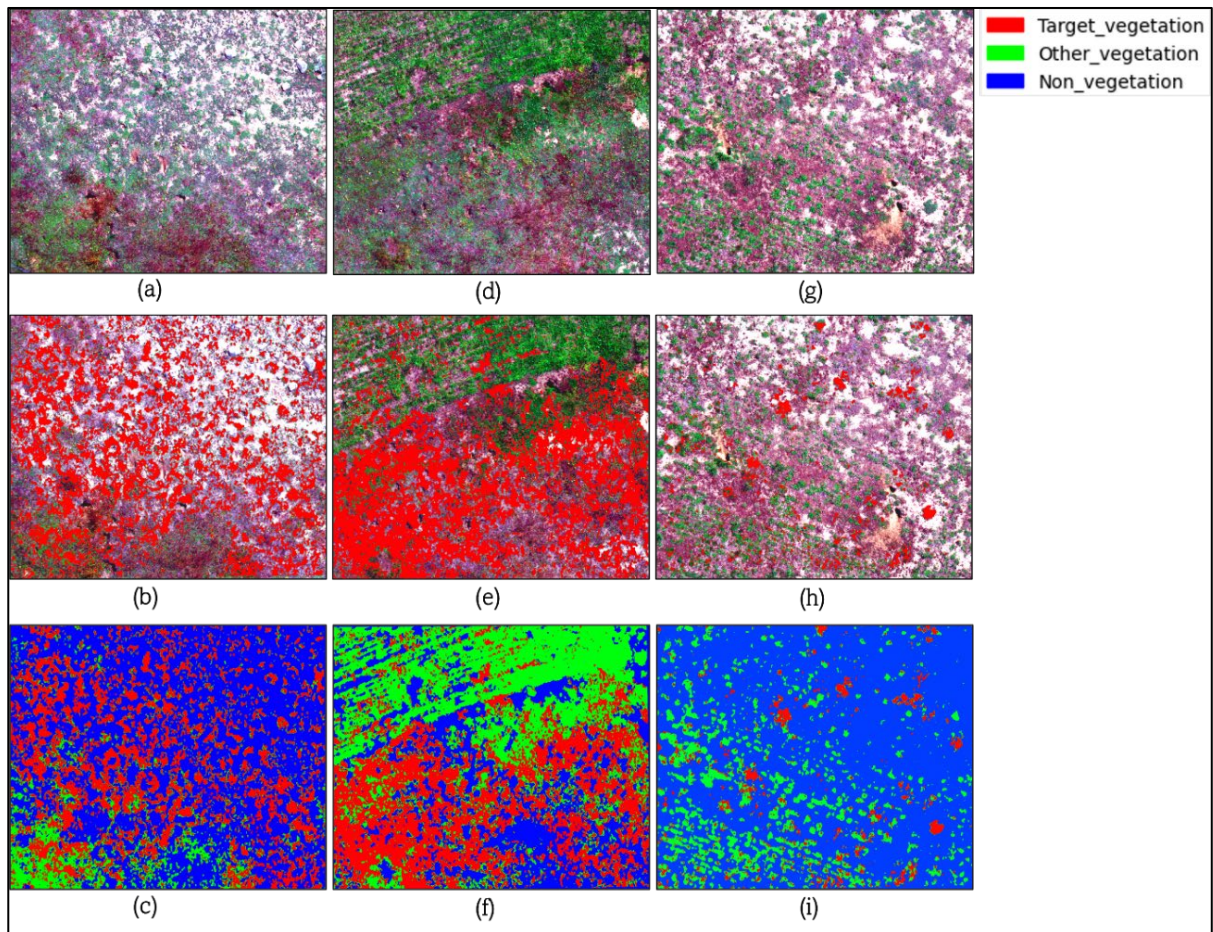


Figure 9: Prediction results at different region of interest (a,d,g)—Different region of study sites; (b,e,h)—Prediction result of hawkweed foliage; (c,f,i)—Prediction results of all classes (Hawkweed foliage, other vegetation, and non-vegetation)

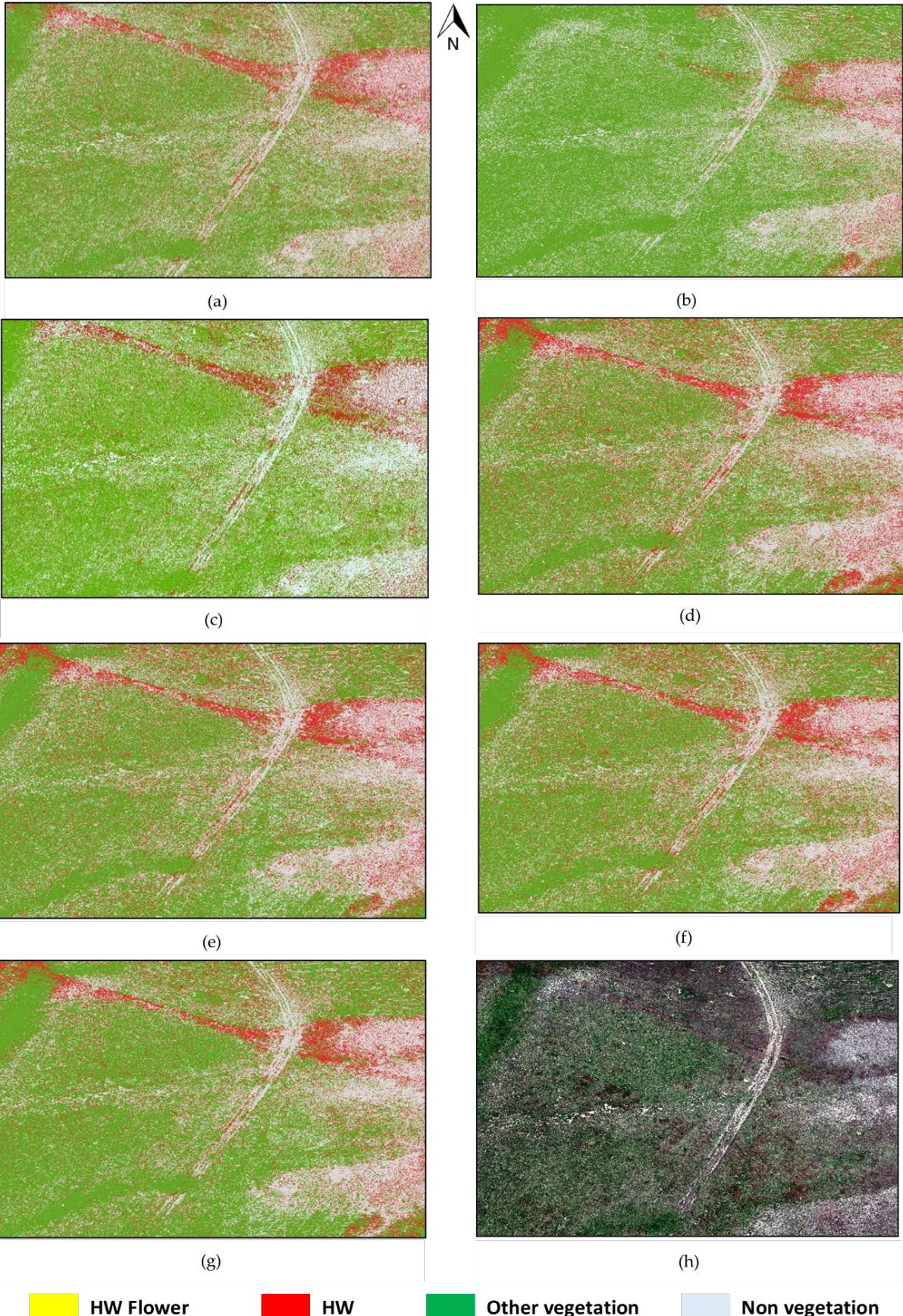


Figure 10: Segmentation results at different GSD (cm/pixel) (a) 0.65; (b) 0.86; (c) 1.10; (d) 1.30; (e) 1.50; (f) 1.73; (g) 1.95; (h) multispectral image.

3.2.2 Fifteen Mile Ridge in NSW

Figures 11 to 16 represent the segmentation results of orange hawkweed, other vegetation, and non-vegetation at different flight missions by the XGBoost model. Due to the poor detection performance of this model, many false positive detections were obtained at different flight missions.

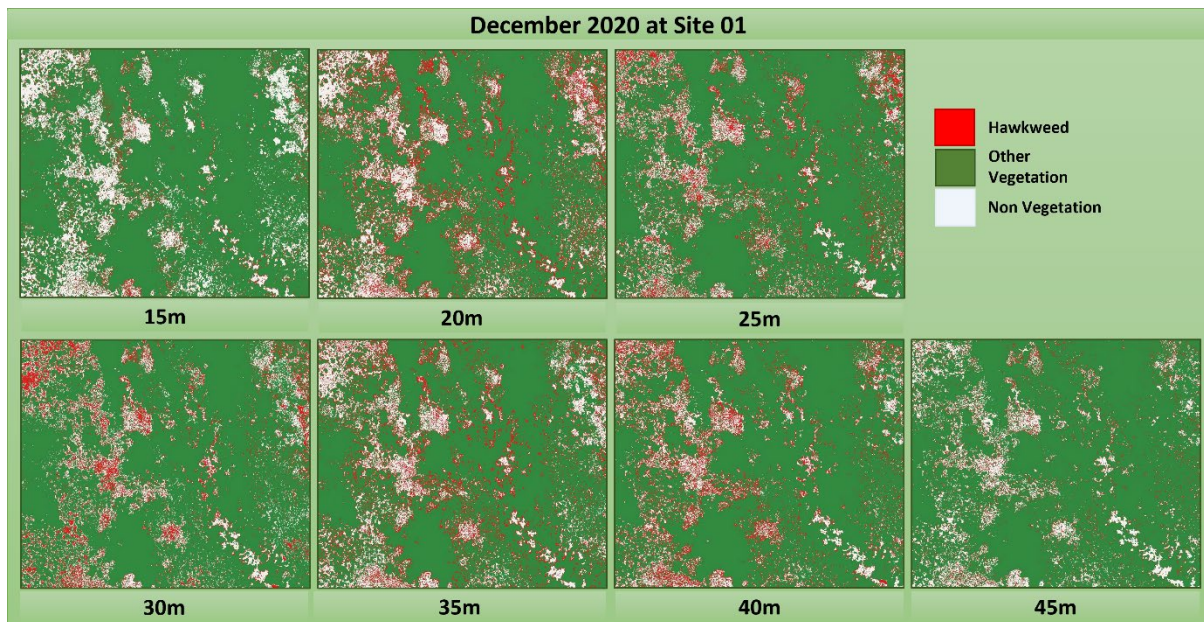


Figure 11: Segmentation results for site 01- December 2020 at different AGL.

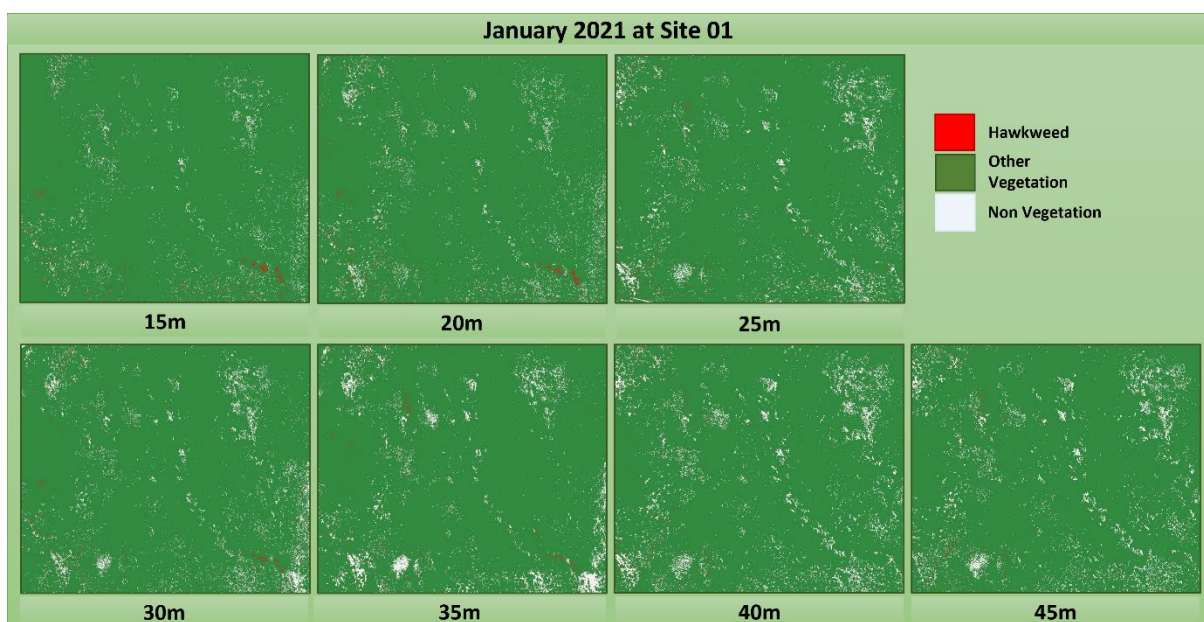


Figure 12: Segmentation results for site 01- January 2021 at different AGL.

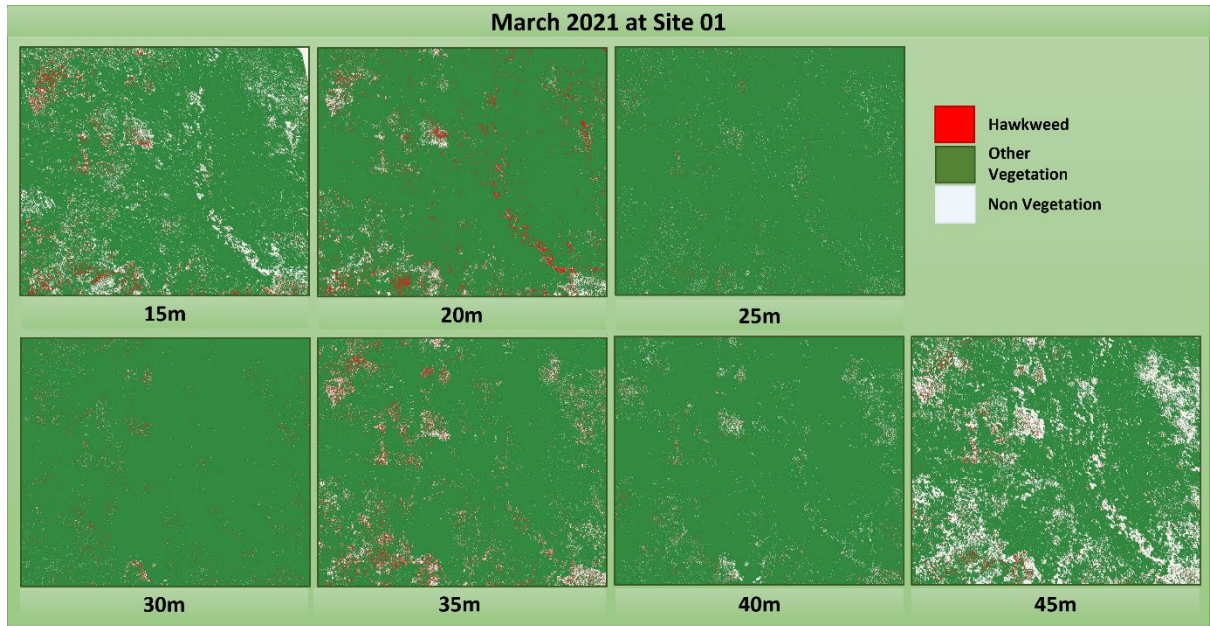


Figure 13: Segmentation results for site 01- March 2021 at different AGL.

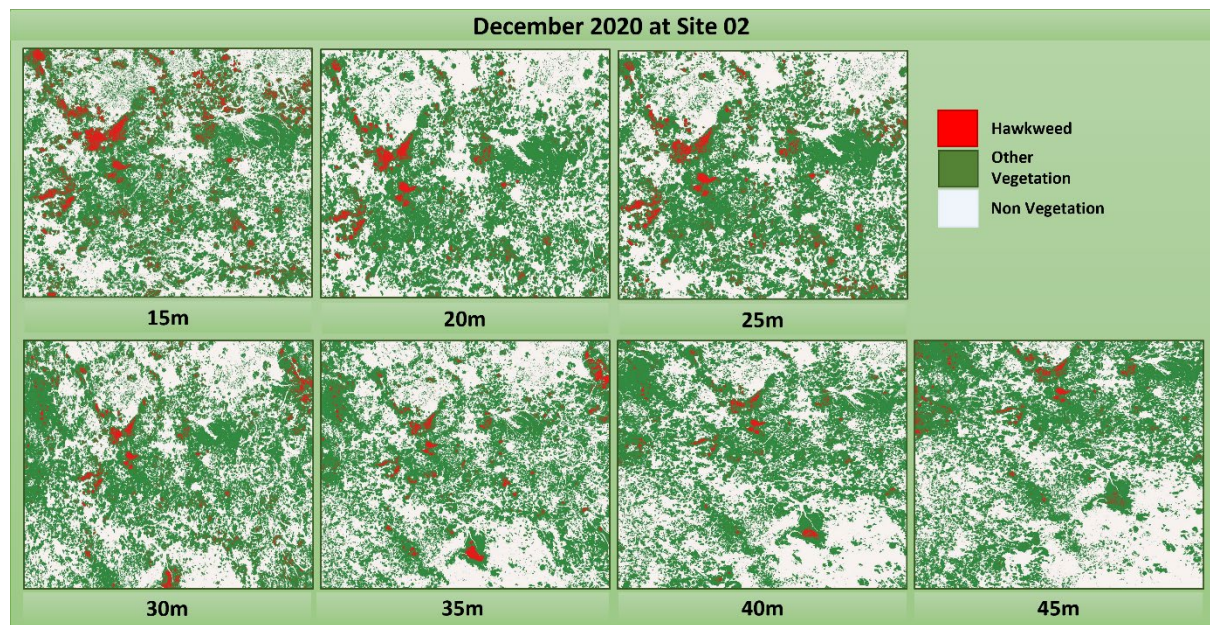


Figure 14: Segmentation results for site 02- December 2020 at different AGL.

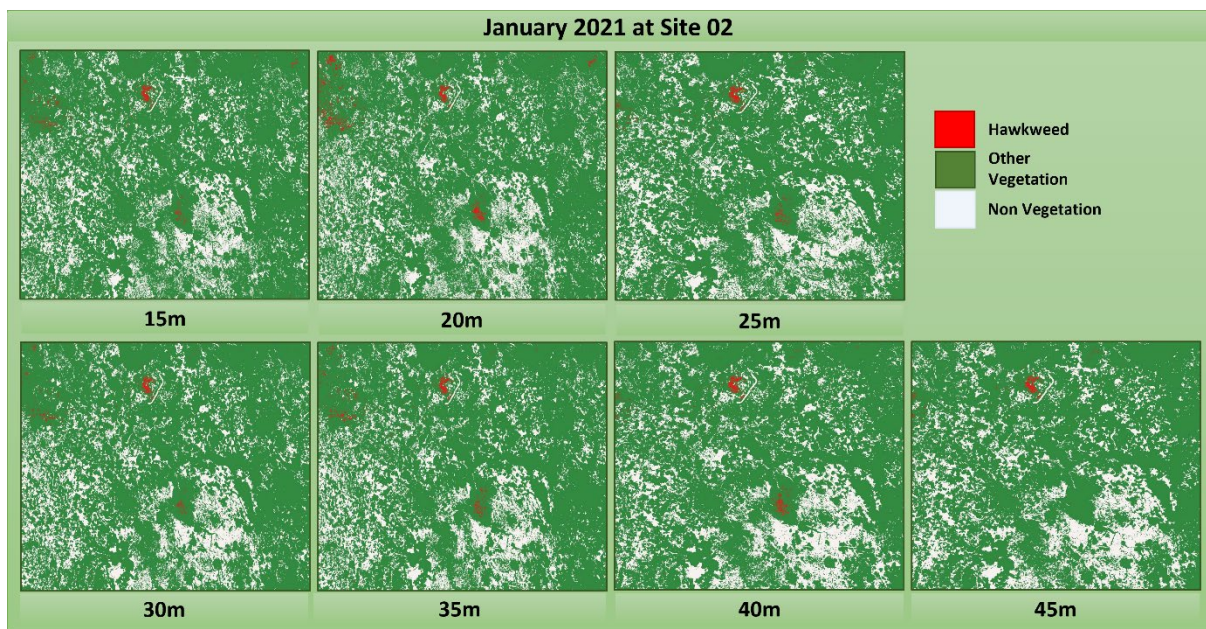


Figure 15: Segmentation results for site 02- January 2021 at different AGL.

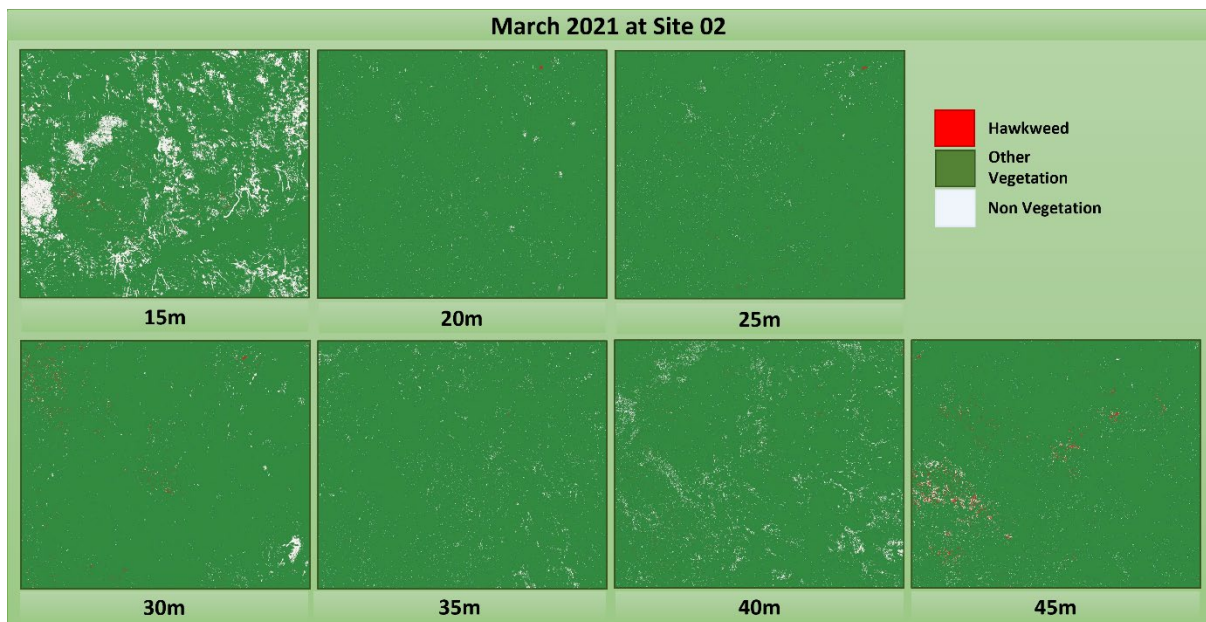


Figure 16: Segmentation results for site 02- March 2021 at different AGL.

Figure 17 represents the temporal variations in orange hawkweed diversity in different sites at 15m AGL during the period between December 2020 and March 2021.

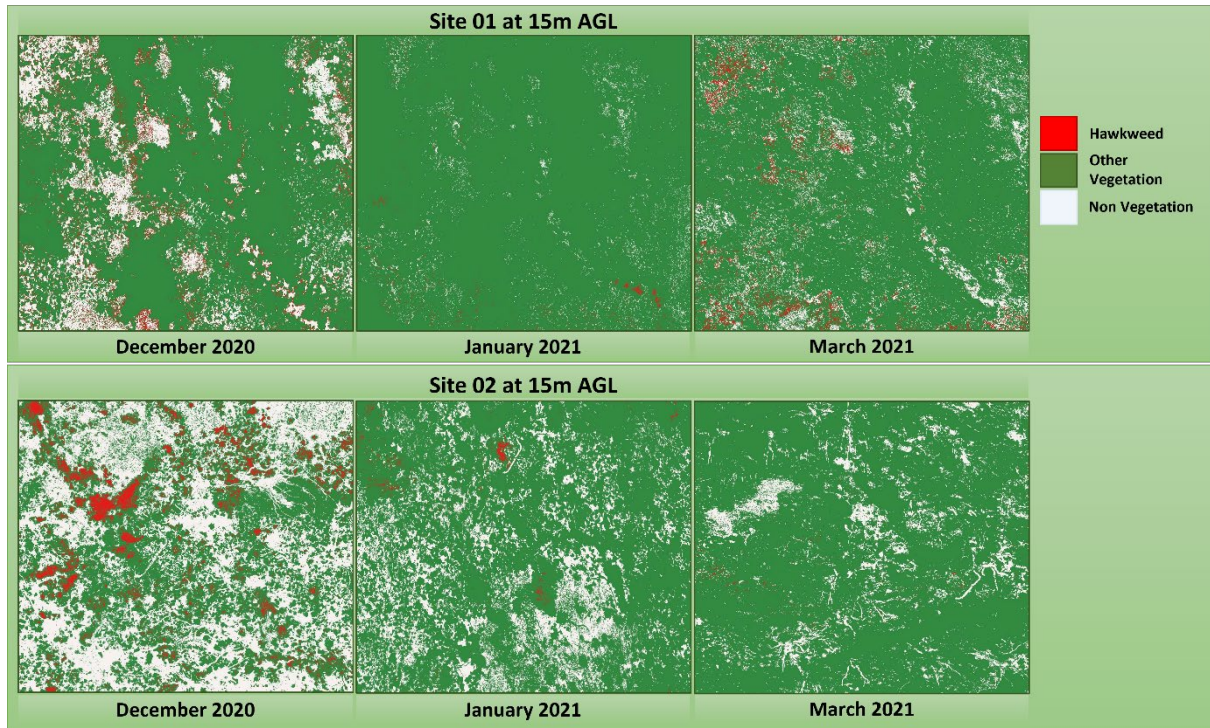


Figure 17: Segmentation results for temporal variation of site 1 at 15m AGL.

3.2.3 Long Plain in NSW

3.2.3.1 Multispectral prediction

Figure 18 represents the segmentation results of hawkweed, hawkweed flower, yellow flower from other vegetation, other vegetation, and non-vegetation at different flight missions by the XGBoost model.

3.2.3.2 Comparison of multispectral and hyperspectral detection

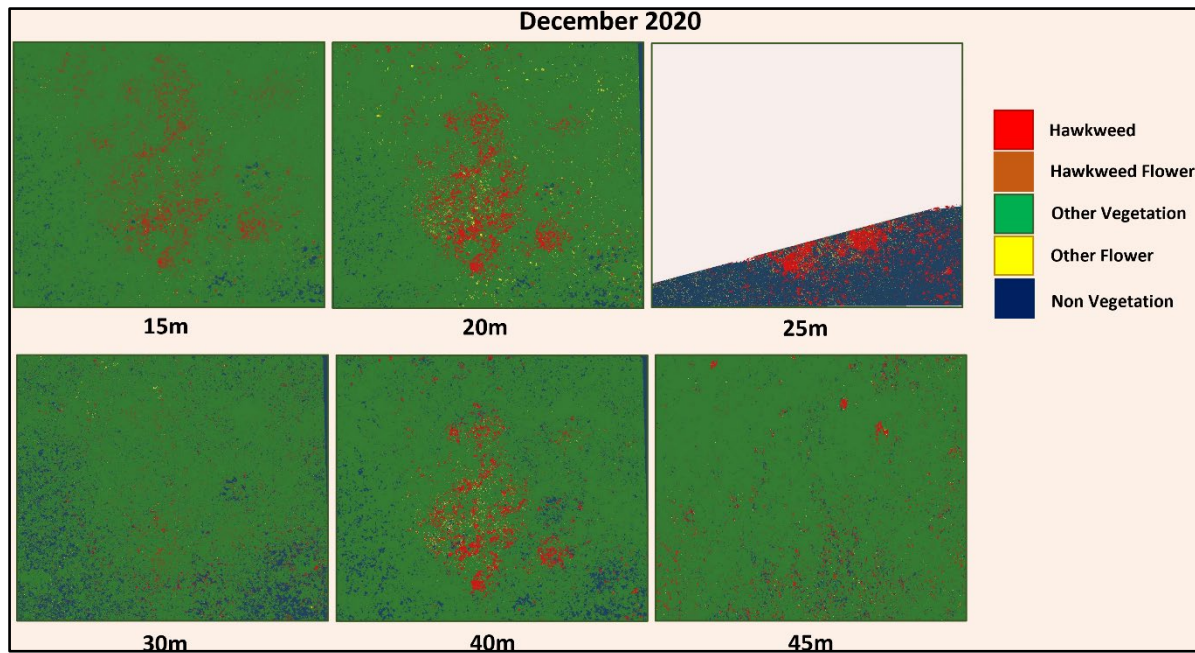


Figure 18: Segmentation results at different AGL.

In addition to these datasets, another set of MS data was collected in December 2021 and obtained a 97% of precision value for the detection of orange hawkweed foliage. The prediction map is displayed on the left side of figure 19. According to the results from MS and HS models,

which produced good detection performance to classify the orange hawkweed foliage. However, the detection of orange hawkweed foliage from the HS dataset can be improved by using more accurate ground truth information with GPS coordinates and the use of spectral information collected from a handheld spectrophotometer for accurate labelling. Moreover, pixel-wise detection of orange hawkweed flowers can be performed by the use of higher spatial resolution HS images.

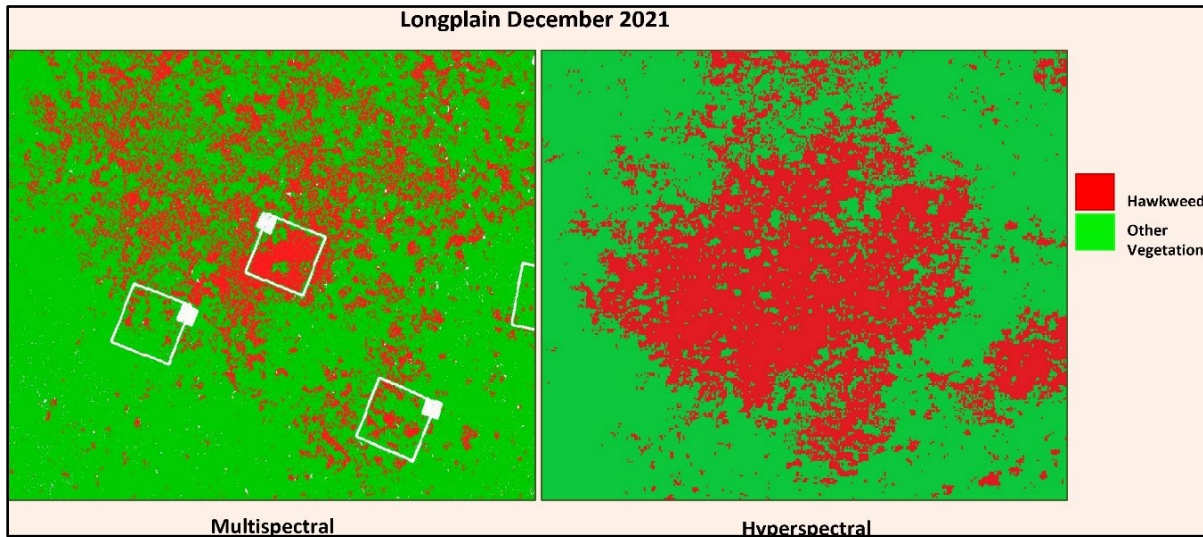


Figure 19: Comparison of MSI and HSI prediction.

4. Discussion

The results of this study indicate the utility of MS and HS sensors installed on UAVs for detecting hawkweed in their flowering or non-flowering stages within a moderately heterogeneous landscape. The preliminary accuracy metrics for the ML model highlight the need for more validation on the prediction of hawkweed using MS and HS imagery within a broader range of vegetation, particularly in a natural context in Australia. When applying ML models to remotely sensed data, the results further demonstrate the importance of spatial resolution to image clarity and detection accuracy. Since acquiring high-resolution data can be expensive, it remains necessary to identify models capable of enhancing image quality and recognising species in lower-resolution imaging. All the main classes (hawkweed flowers, hawkweed foliage, other vegetation, and non-vegetation) can be observed clearly throughout the labelling process using the 15m (0.65cm/pixel) datasets, the greatest resolution.

The XGBoost model achieved the highest overall accuracy compared to other chosen models because it performs effectively with slight to moderate-sized training datasets. However, DT and KNN achieved the lowest overall accuracy since even a small amount of noise can render it unstable, leading to incorrect predictions for the DT model, and KNN is susceptible to noise in the dataset, which can impair the model's accuracy. In addition, the performance of the KNN model is influenced by spatial datasets with a greater dimension. Another intriguing conclusion is that georeferencing techniques are best suited for synchronising aircraft missions with a maximum resolution of 15m and lesser resolutions of 30m to 45m. Detection of hawkweed can be performed with lower resolution imagery if the following techniques can be implemented: 1) higher resolution RGB images are used for labelling the lower resolution MS and HS images; however, it is not a cost-effective method; 2) use of the highest resolution MS and HS image for

labelling the lower resolution rasters; and 3) use of spectral values for labelling the lower resolution rasters which could be a cost-effective way.

5. Benefits of this project

This proposed methodology will provide opportunities for remote weed detection, with the ultimate goal of enabling land managers to target investment and optimise the use of available technologies to detect weeds in the landscape. The findings achieved the following specific benefits.

1. This research proposes a technique for detecting hawkweed using UAV technology mounted with a MS and HS camera and different ML classification algorithms at different spatial resolutions. Therefore, the developed model can be used to detect hawkweed foliage and hawkweed flowers in different flight missions with different spatial resolutions and sites.
2. By saving time for manual labelling, researchers can adopt georeferencing techniques for pixel-wise labelling for lower-resolution imagery.
3. Support effective weed biosecurity and management focused on building capacity and capability in remote weed detection.
4. Provide learning opportunities on remote weed detection current practices and methods.
5. Determining the relationships between accuracy and spatial resolution for study sites will reveal the limits of detection for species and their operational parameters.

6. Limitation of this work

There were a few limitations in this study, as below.

1. One of the important limitations in remote weed detection is the lack of high-resolution RGB images for accurate labelling and the time and expertise required to label images accurately. For small plants like hawkweed, accurate image tagging is difficult without high-resolution RGB imagery or paired ground photos
2. Neighbouring vegetation of similar colour or texture to hawkweed leaves led to some confusion during the labelling process.
3. Hawkweed flower and, to a lesser extent, plant detection accuracy is influenced by the relatively simple floristics of the sampling area, e.g., it is unknown if there were any other similar-coloured (yellow) flowers in the dataset.
4. More clear ground truth information is needed to increase the training sample size to improve the detection models.
5. Some of the other vegetation covered the entire hawkweed location, especially in March 2021. Therefore, there was some confusion during the labelling process.

6. One of the important limitations is the unavailability of the high-resolution HS dataset for the detection of hawkweed flowers.

7. Future works and Recommendations of this project

Future project work will continue to investigate RS technologies and their application to additional model weed systems, including:

1. Increasing ground truth sampling or certainty of training sample identification to improve training samples for better results.
2. Collecting imagery encompassing a greater variety of habitat types (e.g., natural settings) to create a more robust model applicable to a broader range of hawkweed.
3. Collection of more HS imagery to improve model performance and more effectively differentiate between similar vegetative features.
4. Conducting temporal studies to analyse variations in hawkweed density across different seasons and vegetation stages, culminating in the development of a generalised model for predictive analysis.
5. Employing semi-automatic labeling technology to expedite data annotation processes, thereby reducing labor requirements and time expenditure.
6. Leveraging deep learning (DL) segmentation models with transfer learning techniques for training. By utilising transfer learning, we can benefit from pre-trained models and adapt them to our specific task.
7. Exploring advanced data augmentation techniques to augment the training dataset, thereby improving model generalisation and robustness to variations in environmental conditions.
8. Validating accuracy of the segmentation model's predictions through field surveys and ground-truth data collection, ensuring its reliability for practical applications in vegetation management.

8. Conclusions

This study provides a comprehensive overview of the methodologies and objectives undertaken, detailing the analysis of remotely sensed MS and HS imagery of hawkweed in Australia and New Zealand. Utilising pixel-by-pixel classification techniques, our analysis demonstrates the efficacy of MS and HS imagery in accurately and efficiently detecting hawkweed infestations. Among the various ML models evaluated, the XGBoost and RF models emerged as the most effective for detecting hawkweed flowers and foliage at our study locations, thus selected as the optimal approach for training different spatial resolutions of raster images for hawkweed detection. Furthermore, our findings reveal that missions with an altitude of 15m and 20m yielded the highest overall accuracy in identifying hawkweed flowers and foliage. This suggests a correlation

between spatial resolution and detection accuracy, highlighting the importance of considering operational factors in the selection of imaging missions for weed detection applications. In addition to identifying detection limitations for each species based on spatial resolution, this project also addresses the broader implications of remote weed detection in non-crop landscapes. By establishing a CoP for knowledge sharing and information exchange among land managers, we aim to mitigate these limitations and foster collaborative efforts towards effective weed management strategies. In summary, our study contributes valuable insights into the utilisation of RS technology for weed detection, emphasising the importance of tailored approaches and collaborative initiatives in addressing the challenges of invasive species management in diverse ecosystems.

Publication

For more in-depth information, please refer to our research publication: Amarasingam, N., Hamilton, M., Kelly, J. E., Zheng, L., Sandino, J., Gonzalez, F., Dehaan, R. L., & Cherry, H. (2023). Autonomous Detection of Mouse-Ear Hawkweed Using Drones, Multispectral Imagery and Supervised Machine Learning. *Remote Sensing*, 15(6). <https://doi.org/10.3390/rs15061633>.

Acknowledgments

This project is supported through funding from the Department of Agriculture, Fisheries and Forestry grant round (Grant number: 4-FY9LIKQ), Advancing Pest Animal and Weed Control Solutions, as part of the Established Pest Animal and Weeds Pipeline program.

References

- [1] Agriculture Victoria, “Invasive Plants Glossary,” Victorian resource online. Accessed: Apr 08, 2024. [Online]. Available: https://vro.agriculture.vic.gov.au/dpi/vro/vrosite.nsf/pages/weeds_glossary
- [2] E. the E. and W. State of New South Wales (Department of Climate Change, “About pest animals and weeds.” Accessed: Apr. 08, 2024. [Online]. Available: <https://www.environment.nsw.gov.au/topics/animals-and-plants/pest-animals-and-weeds/about-pest-animals-and-weeds#:~:text=Weeds%20smother%20native%20plants%20or,damage%20areas%20of%20cultural%20significance.>
- [3] N. Islam *et al.*, “Early weed detection using image processing and machine learning techniques in an australian chilli farm,” *Agriculture (Switzerland)*, vol. 11, no. 5, 2021, doi: 10.3390/agriculture11050387.
- [4] Calvin Hung and Salah Sukkarieh, “Using robotic aircraft and intelligent surveillance systems for orange hawkweed detection,” *Plant Protection*, vol. 30, no. 3, pp. 100–102, 2015.
- [5] Mark Hamilton, Robert Matthews, and Jo Caldwell, “Needle in a haystack – detecting hawkweeds using drones,” in *21st Australasian Weeds Conference*, 2018, pp. 126–130.
- [6] A. Etienne and D. Saraswat, “Machine learning approaches to automate weed detection by UAV based sensors,” SPIE-Intl Soc Optical Eng, May 2019, p. 25. doi: 10.1117/12.2520536.

- [7] N. Islam *et al.*, “Machine Learning Based Approach for Weed Detection in Chilli Field Using RGB Images,” in *Lecture Notes on Data Engineering and Communications Technologies*, vol. 88, Springer Science and Business Media Deutschland GmbH, 2021, pp. 1097–1105. doi: 10.1007/978-3-030-70665-4_119.
- [8] A. Bakhshipour and A. Jafari, “Evaluation of support vector machine and artificial neural networks in weed detection using shape features,” *Comput Electron Agric*, vol. 145, pp. 153–160, Feb. 2018, doi: 10.1016/j.compag.2017.12.032.
- [9] N.S.G. Williams and K.D. Holland, “The ecology and invasion history of hawkweeds (*Hieracium* species) in Australia,” *Plant Protection*, vol. 22, no. 2, pp. 76–80, 2007.
- [10] “Mouse-ear hawkweed | NSW Environment and Heritage.” Accessed: Jun. 27, 2022. [Online]. Available: <https://www.environment.nsw.gov.au/topics/animals-and-plants/pest-animals-and-weeds/weeds/new-and-emerging-weeds/mouse-ear-hawkweed>
- [11] Mark A. Hamilton, Hillary Cherryand, and Peter J. Turner, “Hawkweed eradication from NSW: Could this be ‘the first’?,” *Plant Protection*, vol. 30, no. 3, pp. 110–115, 2015.
- [12] “Hawkweed | State prohibited weeds | Weeds | Biosecurity | Agriculture Victoria.” Accessed: Jun. 27, 2022. [Online]. Available: <https://agriculture.vic.gov.au/biosecurity/weeds/state-prohibited-weeds/hawkweed>
- [13] A. I. de Castro, J. Torres-Sánchez, J. M. Peña, F. M. Jiménez-Brenes, O. Csillik, and F. López-Granados, “An automatic random forest-OBIA algorithm for early weed mapping between and within crop rows using UAV imagery,” *Remote Sens (Basel)*, vol. 10, no. 2, Feb. 2018, doi: 10.3390/rs10020285.
- [14] N. Department of Primary Industries, *Orange Hawkweed Strategy 2011-2017*. 2011. [Online]. Available: www.dpi.nsw.gov.au/
- [15] Nicholas Williams, Amy Hahs, John Morgan, and Kelly Holland, “A dispersal constrained habitat suitability model for orange hawkweed (*Hieracium aurantiacum*) on the Bogong high plains, victoria,” Melbourne, 2007.
- [16] T. Kompas, L. Chu, and H. T. M. Nguyen, “A practical optimal surveillance policy for invasive weeds: An application to Hawkweed in Australia,” *Ecological Economics*, vol. 130, pp. 156–165, Oct. 2016, doi: 10.1016/j.ecolecon.2016.07.003.